The *C. elegans* DYRK Kinase MBK-2 Marks Oocyte Proteins for Degradation in Response to Meiotic Maturation

Michael L. Stitzel,[1,2] Jason Pellettieri,[1,3]
and Geraldine Seydoux[1,2,*]
[1] Howard Hughes Medical Institute and
Department of Molecular Biology and Genetics
[2] Predoctoral Training Program in Human Genetics
Johns Hopkins School of Medicine
725 N. Wolfe St., PCTB 706
Baltimore, Maryland 21205

Summary

The oocyte-to-embryo transition transforms a differentiated germ cell into a totipotent zygote capable of somatic development. In *C. elegans*, several oocyte proteins, including the meiotic katanin subunit MEI-1 and the oocyte maturation protein OMA-1, must be degraded during this transition [1]. Degradation of MEI-1 and OMA-1 requires the dual-specificity YAK-1-related (DYRK) kinase MBK-2 [2–4]. Here, we demonstrate that MBK-2 directly phosphorylates MEI-1 and OMA-1 in vitro and that this activity is essential for degradation in vivo. Phosphorylation of MEI-1 by MBK-2 reaches maximal levels after the meiotic divisions, immediately preceding MEI-1 degradation. MEI-1 phosphorylation and degradation still occur in *spe-9* eggs, which undergo meiotic maturation and exit in the absence of fertilization [5]. In contrast, MEI-1 phosphorylation and degradation are blocked in cell-cycle mutants that arrest during the meiotic divisions, and are accelerated in *wee-1.3(RNAi)* oocytes, which prematurely enter meiotic M phase (A. Golden, personal communication). A GFP:MBK-2 fusion relocalizes from the cortex to the cytoplasm during the meiotic divisions, and this relocalization also depends on cell-cycle progression. Our findings suggest that regulators of meiotic M phase activate a remodeling program, independently of fertilization, to prepare eggs for embryogenesis.

Results

MBK-2's Kinase Activity Is Essential In Vivo

To characterize the kinase activity of MBK-2, we first tested whether recombinant MBK-2 could phosphorylate a synthetic peptide (DYRKtide) containing the DYRK target consensus $RX_{1-3}S/TP$ [6, 7]. Wild-type MBK-2, but not mutant MBK-2 with a mutation in the predicted ATP binding site (K196R), could phosphorylate DYRKtide (Figure 1A), consistent with MBK-2 possessing the kinase activity typical of the DYRK family. To determine if kinase activity is essential in vivo, we tested whether MBK-2 and MBK-2(K196R), when fused to green fluorescent protein (GFP), could complement the deletion allele *mbk-2(pk1427)* [3]. Embryos derived from *mbk-2(pk1427)*

mothers are not viable (0% viability n = 1063). Wild-type GFP:MBK-2 restored viability to 80% (n = 569); in contrast, GFP:MBK-2(K196R) did not rescue (0% viability, n = 198). GFP:MBK-2 and GFP:MBK-2(K196R) were expressed at comparable levels (Figure S1 in the Supplemental Data available with this article online) and in similar patterns (Figure 1B). The only difference was that GFP:MBK-2(K196R) localized to the meiotic spindle in metaphase of meiosis I (Figure 1B_f, arrowhead, 37/66 embryos), whereas GFP:MBK-2 did not (0/43 embryos). We conclude that kinase activity, although not essential for most aspects of GFP:MBK-2 localization, is essential for MBK-2 function in vivo.

MBK-2 Directly Phosphorylates MEI-1 and OMA-1 In Vitro on Sites Required for Degradation In Vivo

Next, we tested whether recombinant MBK-2 could phosphorylate MEI-1, OMA-1, and POS-1, three proteins that require MBK-2 for degradation in vivo [2–4]. MBP:MBK-2 could phosphorylate MBP:MEI-1 and MBP:OMA-1, but neither MBP:POS-1 nor MBP alone (Figure 1C). MBK-2 (K196R) did not phosphorylate any target, confirming that MBK-2 is the active kinase in this assay (Figure S2A).

MEI-1 and OMA-1 contain one and two $RX_{1-3}S/TP$ consensus sites, respectively, whereas POS-1 does not contain any (Figure S2B and data not shown). In MEI-1 and OMA-1, one copy of the consensus overlaps with a PEST sequence, a motif commonly found in proteins with high turnover [8]. Disruption of these DYRK sites [MEI-1(S92A) and OMA-1(P240L)] reduced MBK-2's ability to phosphorylate each substrate (Figure 1C). We conclude that MBK-2 can phosphorylate MEI-1 and OMA-1 on DYRK consensus sites embedded in PEST sequences (also see below).

OMA-1(P240L) exhibits increased protein stability in vivo and causes embryonic lethality [9, 10], suggesting that phosphorylation by MBK-2 is required for OMA-1 degradation. To test whether phosphorylation by MBK-2 is also required for MEI-1 degradation, we examined the distribution of MEI-1(S92A) fused to GFP. To avoid the lethality associated with failure to degrade MEI-1, we introduced a second mutation, R36C, to knock out MEI-1 catalytic activity [11, 12]. Like wild-type MEI-1, GFP:MEI-1(R36C) was rapidly degraded during the transition from meiosis to mitosis (Figure 1D). In contrast, GFP:MEI-1(R36C,S92A) was maintained past the first mitotic division (Figure 1D). We conclude that MBK-2 consensus sites in MEI-1 and OMA-1 are required for timely degradation in vivo.

Phosphorylation of MEI-1 by MBK-2 Precedes Degradation In Vivo

To investigate the dynamics of MEI-1 phosphorylation in vivo, we generated an antibody specific for MEI-1 phosphorylated on S92 (P-MEI-1; see Experimental Procedures). Antibody specificity was confirmed with western blots of in vitro-phosphorylated proteins (Figure 2A) and by comparing immunostained wild-type embryos and mutant embryos lacking MEI-1 or MBK-2 (Table S1).

*Correspondence: gseydoux@jhmi.edu
[3] Present address: Neurobiology and Anatomy, University of Utah, MREB Rm 401, Salt Lake City, Utah 84112.
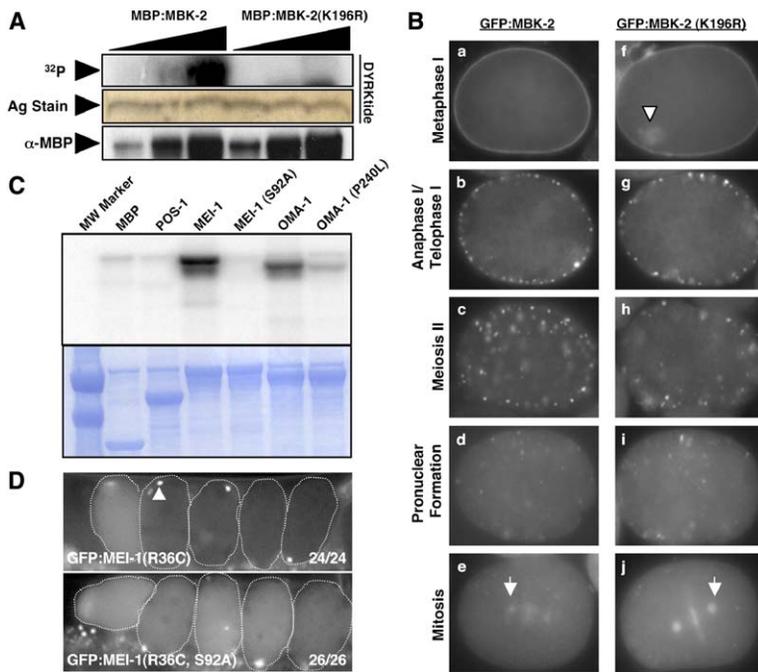
Figure 1. In Vitro and In Vivo Properties of Wild-Type and Kinase-Inactive (K196R) MBK-2

(A) In vitro phosphorylation of DYRKtide by MBK-2. Serial 3-fold dilutions of MBP:MBK-2 fusions were incubated with 1 μM DYRKtide in the presence of γ-^{32}P-ATP (top). Equal loading of DYRKtide was confirmed by silver (Ag) stain (middle). MBP:MBK-2 amounts in each reaction were confirmed by α-MBP western blot (bottom).

(B) In vivo localization of GFP:MBK-2 and GFP:MBK-2(K196R) in mbk-2(pk1427) mutants. Live embryos expressing wild-type (B$_{a–e}$) or kinase-inactive (K196R) (B$_{f–j}$) GFP:MBK-2. Both fusions are found on the periphery (cortex) of oocytes (B$_a$ and B$_f$), coalesce into cortical puncta of unknown identity by anaphase I (B$_b$ and B$_g$), internalize, and dissipate into the cytoplasm as meiosis progresses and is completed (B$_{c–d}$ and B$_{h–i}$). At mitosis, each fusion is predominantly cytoplasmic and accumulates on the mitotic spindle and chromatin (B$_e$ and B$_j$). The arrowhead in B$_f$ points to GFP:MBK-2(K196R) on the meiotic spindle; arrows show examples of GFP:MBK-2 on centrosomes. Embryos are oriented with anterior to the left and posterior to the right.

(C) MBK-2 phosphorylates MEI-1 and OMA-1 directly in vitro. MBP:MBK-2 was incubated with the indicated MBP fusions in kinase buffer with γ-^{32}P-ATP, run on a NuPAGE 4%–12% Bis-Tris gel (Invitrogen), and stained with Simply Blue SafeStain (lower panel, Invitrogen). A Phosphoimager was used to detect ^{32}P incorporation (upper panel). The faint band present in the MBP, POS-1, and MEI-1(S92A) lanes is autophosphorylated MBP:MBK-2. MW denotes molecular weight.

(D) S92 is required for MEI-1 degradation in vivo. Fluorescence of live embryos in the uterus of hermaphrodites expressing GFP:MEI-1 (R36C) (top) or GFP:MEI-1(R36C, S92A) (bottom) is shown. Dotted lines outline embryos that are arranged, youngest to oldest, from left to right. The arrowhead in the top panel marks an example of GFP:MEI-1 in a polar body. Numbers indicate the number of gonad arms exhibiting the expression patterns shown/total number of gonadal arms examined. Fluorescence below the embryos is due to autofluorescence of the hermaphrodite gut.

P-MEI-1 was first detected on the maternal chromatin in anaphase of meiosis I (Figure 2B$_g$, open arrowhead, and Table S2). P-MEI-1 in the cytoplasm was first detected during meiosis II and reached peak levels during pronuclear formation (meiotic exit; Figure 2B$_{h–i}$). P-MEI-1 levels dropped sharply between pronuclear formation and the first cell division (Figure 2B$_{i–j}$), except in the polar bodies (filled arrowhead, Figure 2B$_{h–j}$). Comparison of the relative cytoplasmic intensities of GFP:MEI-1 and P-MEI-1 revealed that (1) the sharp increase in P-MEI-1 levels precedes the decline of GFP:MEI-1 and (2) the disappearance of P-MEI-1 coincides with disappearance of GFP:MEI-1 (Figure 2C). Consistent with loss of P-MEI-1 being due to degradation, P-MEI-1 levels remained steady in mel-26(RNAi) embryos, which do not degrade MEI-1 (data not shown). We conclude that phosphorylation of MEI-1 by MBK-2 closely precedes MEI-1 degradation in vivo.

Cell-Cycle Dependence of MEI-1 Phosphorylation and MEI-1 and OMA-1 Degradation

In the absence of sperm, C. elegans oocytes arrest in prophase of meiosis I [13]. The sperm-derived MSP peptide activates oocyte maturation, ovulation, and the first meiotic division in the oocyte closest to the spermatheca [14]. Fertilization triggers the second meiotic division and the switch to mitosis [5]. To determine which of these events is required to activate MEI-1 and OMA-1 degradation, we examined mutants defective in fertilization or meiotic progression. We describe results here for

GFP:MEI-1, but have also obtained similar data for OMA-1:GFP (data not shown).

spe-9(hc52) hermaphrodites contain sperm that stimulate oocyte maturation but do not fertilize oocytes [15, 16]. Oocytes are ovulated and reach anaphase of the first meiotic division, but eventually exit the meiotic cell cycle without extruding a polar body or forming a meiosis II spindle [5]. We found that GFP:MEI-1 was degraded shortly after ovulation in spe-9(hc52) hermaphrodites (Figure 3B). This degradation was dependent on MBK-2, because it was blocked when MBK-2 was depleted by RNAi (Figure 3C). Furthermore, we detected robust P-MEI-1 in ovulated spe-9(hc52) eggs with decondensing chromatin (Figure 3K). We conclude that fertilization and the second meiotic division are not required for MEI-1 phosphorylation or degradation.

Hermaphrodites that lack the cell-cycle regulators CDK-1 (cyclin-dependent kinase) and MAT-1 (anaphase-promoting complex/cyclosome [APC/C] subunit) ovulate and fertilize oocytes that arrest in prophase of meiosis I (cdk-1) or in metaphase of meiosis I (mat-1) [17–19]. In both cases, we found that GFP:MEI-1 was not degraded in the arrested embryos (Figures 3D and E). In addition, we did not detect P-MEI-1 in mat-1(RNAi) embryos (Figure 3L). We conclude that arrest before anaphase I is sufficient to block MEI-1 phosphorylation and degradation even in the presence of fertilization.

Depletion of the cullin CUL-2 and the leucine-rich repeat protein ZYG-11 by RNAi delays metaphase of meiosis II for 30–40 min before zygotes eventually exit
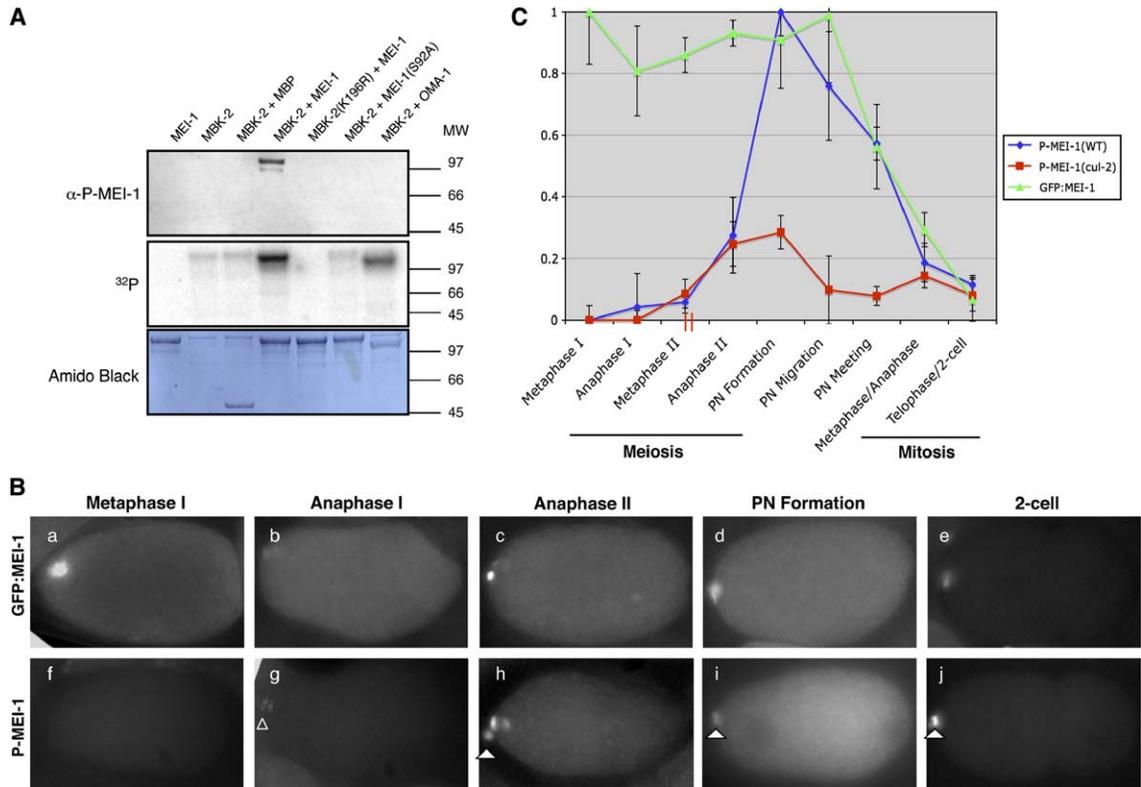
Figure 2. MEI-1 Is Phosphorylated by MBK-2 at S92 In Vivo Prior to Its Degradation

(A) α-P-MEI-1 antibody specifically recognizes S92-phosphorylated MEI-1 in vitro. The indicated MBP fusion proteins were incubated in kinase buffer with unlabeled ATP or γ-^{32}P ATP. Reaction products were separated as in Figure 1C, and phosphorylated MEI-1 was detected with α-P-MEI-1 (1:2000 dilution; Experimental Procedures) after transfer to a nitrocellulose membrane (top) or ^{32}P incorporation was measured as in Figure 1C (γ-^{32}P ATP, middle). Equal loading for the western was confirmed by amido-black staining of the membrane (bottom). MW denotes molecular weight, expressed in kD.

(B) Dynamics of MEI-1 phosphorylation in vivo. Fixed embryos at the indicated stages expressing GFP:MEI-1 (B$_{a-e}$) or stained with α-phospho-MEI-1 antibody (B$_{f-j}$) are shown. P-MEI-1 is first detected on the chromatin at anaphase of Meiosis I (B$_g$, open arrowhead; see also Table S2). P-MEI-1 staining was also detected in polar bodies (B$_{h-j}$, arrowheads). PN denotes pronuclear.

(C) Graph of GFP:MEI-1 and P-MEI-1 levels in wild-type and cul-2(RNAi) embryos from metaphase of meiosis I through the 2-cell stage. Two vertical red lines on the x axis represent the point in meiosis where cul-2(RNAi) mutants temporarily arrest. Values plotted are the mean value ± standard error (see Experimental Procedures). PN denotes pronuclear.

meiosis and switch to mitosis [20, 21]. Consistent with this temporary arrest, we found that GFP:MEI-1 degradation was delayed in cul-2(RNAi) embryos (Figure 3F) and zyg-11(RNAi) embryos (62/68 gonadal arms examined, data not shown). P-MEI-1 levels in metaphase II-arrested cul-2(RNAi) embryos were low and comparable to those measured in wild-type embryos at the same stage (Figure 2C). Furthermore, cul-2 embryos that progressed past the meiosis II arrest reached only one-third the level of P-MEI-1 compared to wild-type embryos (Figure 2C). These results suggest that timely progression through meiosis is required to induce a burst of MEI-1 phosphorylation.

To test whether meiotic progression is sufficient to stimulate MEI-1 degradation, we examined hermaphrodites depleted for the negative regulator WEE-1.3. WEE-1.3 is the C. elegans Myt1 kinase, which inhibits CDK-1 activity by phosphorylation [22]. wee-1.3(RNAi) causes oocytes in the proximal gonad to prematurely enter meiotic M phase (A. Golden, personal communication). We found that GFP:MEI-1 was degraded prematurely in the gonad of wee-1.3(RNAi) hermaphrodites (Figure 3G). Furthermore, we detected P-MEI-1 in unovulated

oocytes in 9/13 wee-1.3(RNAi) gonads (Figure 3M) compared to 0/19 wild-type gonads (data not shown). Premature degradation of GFP:MEI-1 in wee-1.3(RNAi) was dependent on MBK-2 and meiotic progression, because it could be blocked by also depleting MBK-2, CDK-1, or MAT-1 (Figures 3H–3J). Taken together, these data suggest that precocious meiotic progression is sufficient to activate MEI-1 phosphorylation and degradation.

Cell-Cycle Dependence of GFP:MBK-2 Dynamics

GFP:MBK-2 relocalizes abruptly from the cortex to cortical puncta in anaphase/telophase of meiosis I [3, 5] and progressively from cortical puncta to the cytoplasm during meiosis II and meiotic exit (Figure 1B$_{a-d}$). Consistent with two distinct steps of relocalization, embryos arrested before or during metaphase I maintain GFP:MBK-2 uniformly at the cortex (Figures 4B and 4C and [3]), whereas embryos arrested in metaphase II maintain GFP:MBK-2 in cortical puncta, with some puncta in the cytoplasm (Figure 4D and 20/24 zyg-11(RNAi) gonads, data not shown). In spe-9 eggs, GFP:MBK-2 progressed from the cortex into cortical puncta and the cytoplasm as in wild-type embryos, suggesting that meiotic exit,
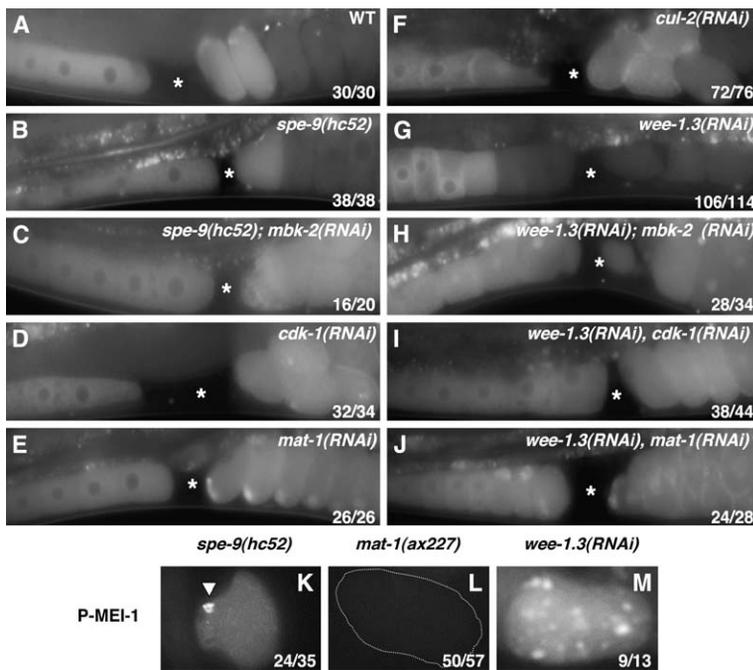
Figure 3. Meiotic Maturation, Not Fertilization, Is Required for MEI-1 Phosphorylation and Degradation

(A–J) Fluorescence photomicrographs of oocytes and embryos expressing GFP:MEI-1 in hermaphrodites with the indicated genotypes. The spermatheca is indicated by an asterisk; oocytes are to the left, embryos to the right. Both are arranged, youngest to oldest, from left to right. Numbers refer to the number of gonadal arms with phenotype shown/total number of gonadal arms examined. Exceptional arms were consistent with incomplete penetrance of the RNAi treatment.

(K–M) Fixed embryos or oocytes of the indicated genotype stained with α-phospho-MEI-1. The localized high concentration of P-MEI-1 in spe-9(hc52) (arrowhead in [K]) corresponds to the maternal chromatin as detected by DAPI (not shown). Numbers in (K) and (L) indicate the number of eggs with the phenotype shown/total number examined. Numbers in (M) refer to the number of gonadal arms with at least one P-MEI-1-positive oocyte/total number of gonadal arms examined.

rather than meiosis II, is critical (Figure 4E and [5]). In *wee-1.3(RNAi)* oocytes, relocalization of GFP:MBK-2 to cortical puncta and to the cytoplasm occurred precociously in oocytes (Figure 4F and A. Golden, personal communication). This premature relocalization was blocked by CDK-1 and MAT-1 depletion (Figures 4G and 4H). We conclude that GFP:MBK-2 relocalizes from the cortex to the cytoplasm in a two-step process linked to progression past metaphase I and possibly to meiotic exit.

Discussion

Phosphorylation by MBK-2 Marks Oocyte Proteins for Degradation

Several observations support the hypothesis that phosphorylation by MBK-2 triggers MEI-1 degradation at meiotic exit. First, MBK-2 phosphorylates MEI-1 on S92 directly in vitro. Second, S92 is phosphorylated in vivo, and this phosphorylation requires MBK-2. Third, S92

phosphorylation immediately precedes MEI-1 degradation. Finally, substitution of S92 with the nonphosphorylatable amino acid alanine blocks MEI-1 degradation.

How does phosphorylation stimulate MEI-1 destruction? Degradation of MEI-1 depends on recognition by MEL-26, the substrate recruitment factor for the E3 ubiquitin ligase MEL-26/CUL-3 [1]. The expression pattern of MEL-26 is not yet known, but one possibility is that phosphorylation by MBK-2 increases the affinity of MEI-1 for MEL-26 or the MEL-26/CUL-3 complex at meiotic exit. For example, phosphorylation of Sic1p by cyclin/Cdk stimulates its recognition by Cdc4p during the G1/S transition in *S. cerevisiae* [23]. Whether MEI-1 needs to be phosphorylated to interact with MEL-26 in vivo remains to be determined.

MBK-2 also phosphorylates OMA-1 in vitro on a site essential for degradation in vivo, suggesting that OMA-1 is a second MBK-2 target. Nishi and Lin [24] and Shirayama et al. (published online in *Current Biology* December 8, 2005, [25]) independently have obtained similar
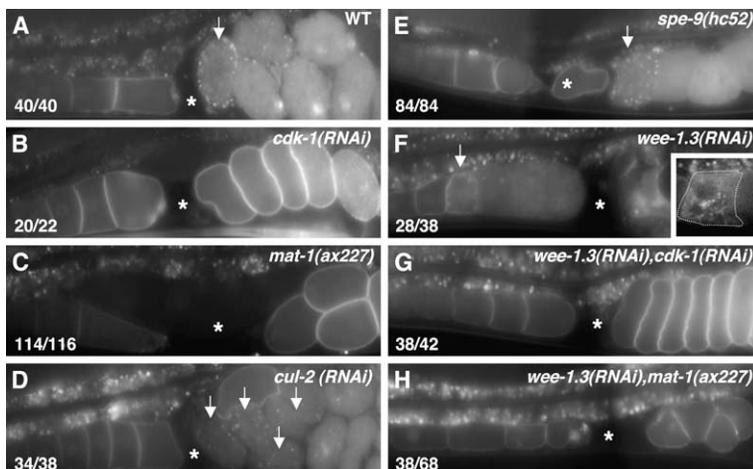

Figure 4. Meiotic Maturation, Not Fertilization, Is Required for GFP:MBK-2 Redistribution

(A–H) Fluorescence photomicrographs of oocytes and embryos expressing GFP:MBK-2 in hermaphrodites with the indicated genotypes. Oocytes and embryos are arranged as described in Figure 3. Arrows point to oocytes or embryos with MBK-2 puncta. An enlarged surface view of the oocyte marked by an arrow in (F) is shown in the inset. Numbers refer to the number of gonadal arms with phenotype shown/total number of gonadal arms examined. Exceptional arms were consistent with incomplete penetrance of the RNAi treatment or incomplete penetrance of the temperature-sensitive allele *mat-1(ax227)*.

results. Additionally, Nishi and Lin have demonstrated that OMA-1 phosphorylation occurs in vivo and peaks at meiotic exit [24], just as we report here for MEI-1. Unlike MEI-1, however, OMA-1 is not degraded until after the first mitosis. Consistent with this delay, OMA-1 degradation also requires phosphorylation by a second kinase [24].

The human DYRK kinase DYRK1B/Mirk has also been reported to destabilize target proteins. During differentiation of C2C12 myoblasts, DYRK1B/Mirk phosphorylates cyclin D1, leading to its destruction and G_0/G_1 cell-cycle arrest [26]. Other DYRK1B/Mirk targets, however, have been reported to become stabilized or to change localization following phosphorylation [27–29]. Together with our findings, these studies suggest that a common role for DYRK kinases may be to facilitate developmental transitions by modifying the stability and/or localization of multiple target proteins in differentiating cells.

Activators of Meiotic M Phase Stimulate Oocyte-Protein Degradation

Transition from an oocyte to an embryo requires completion of the meiotic divisions and fertilization. In most animals, oocytes are released from prophase arrest by maturation and progress until a second arrest point (typically metaphase I or II), pending fertilization [30]. Calcium signaling at fertilization releases oocytes from this second arrest, allowing completion of the meiotic divisions and meiotic exit [31]. In this respect, C. elegans differs from most commonly studied model systems because fertilization is not required for meiotic exit [5]. Unfertilized, matured oocytes arrest temporarily in anaphase I, but eventually exit meiosis without forming a second meiotic spindle [5]. This unusual property allowed us to determine whether meiosis or fertilization is most directly required for MBK-2-dependent events. We found that meiotic maturation, rather than fertilization, is necessary and sufficient to induce MEI-1 phosphorylation and degradation. At this point, we do not know whether MEI-1 phosphorylation is activated as a secondary consequence of meiotic maturation or depends more directly on a specific cell-cycle activator of meiotic M phase. MEI-1 phosphorylation is first detected on the meiotic spindle in anaphase of meiosis I, with peak levels reached by meiotic exit. OMA-1 phosphorylation also first peaks at meiotic exit [24], suggesting that this timing is specified by a property intrinsic to MBK-2 rather than its substrates.

How is MBK-2 activated during meiotic progression? A GFP:MBK-2 fusion relocalizes from the cortex, to cortical puncta, and to the cytoplasm during the meiotic division. Because MEI-1 and OMA-1 are both cytoplasmic proteins, an attractive possibility is that release of MBK-2 from the cortex allows it to reach its targets. Examination of the localization dynamics of endogenous MBK-2 will be necessary before this hypothesis can be explored further. Nevertheless, the finding that GFP:MBK-2 relocalizes in a cell-cycle-dependent manner supports the view that meiotic progression elicits significant changes throughout the egg. We suggest that the meiotic cell-cycle machinery activates an egg-wide remodeling program that facilitates the transition from a differentiated germ cell to a totipotent zygote.

Experimental Procedures

Nematode Strains, Lethality Analysis, and Temperature-Shift Experiments

C. elegans strains (Table S3) were derived from the wild-type Bristol strain N2 and reared with standard procedures [32]. mat-1(ax227) and spe-9(hc52) hermaphrodites were maintained at 16ºC and shifted to 25ºC as L4 larvae and as embryos, respectively.

RNAi-Mediated Interference

RNAi-mediated interference (RNAi) was performed with the feeding method [33], as described in [3, 34]. cdk-1, mat-1, wee-1.3, and mel-26 RNAi clones were obtained from the Ahringer RNAi library [35], cul-2 from [36], and mbk-2 from [3].

Cloning and Transgenics

Gateway cloning (Invitrogen) was used to generate all constructs [37]. Coding sequences were PCR amplified from cDNA and cloned into pDONR201. pDONR constructs were recombined into pID3.01B (for N-terminal GFP fusion proteins), pCD1.01 (for RNAi feeding experiments), or pJP1.09 (for N-terminal maltose binding protein fusions). Point mutations in the MEI-1 and OMA-1 coding sequences were introduced in the pDONR constructs with the QuikChange Site-Directed Mutagenesis Kit (Stratagene). GFP lines were generated by the microparticle bombardment method [38].

Expression and Partial Purification of MBP Fusion Proteins

MBP fusions were grown in E. coli strain CAG456 and induced with 300 µM isopropyl-β-D-1-thiogalactopyranoside (IPTG) overnight at 15ºC. Bacterial pellets were washed and resuspended in 10 ml ice-cold column buffer (20 mM Tris-HCl, 500 mM NaCl, 1 mM EDTA, 1 mM 1,4-Dithio-DL-threitol [DTT], 10% glycerol), passed once through a French Press, and centrifuged (SW41 rotor at 36,000 RPM, SA300 rotor at 20,000 RPM, or equivalent, for 30 min).

MBP fusions were partially purified from cleared lysates by affinity chromatography (amylose resin, New England Biolabs) and eluted with 250 µl column buffer plus 10 mM maltose. Eluates were stored at −80ºC. Kinase assays were performed as in [39].

Immunoblotting

One hundred and twenty-five hermaphrodites for each genotype in Figure S1 were collected into 7.5 µl distilled water and frozen in a dry-ice/ethanol bath. Two and a half microliters of 4× NuPAGE LDS sample buffer and 0.5 µl 1M DTT were added to each tube, and the samples were boiled at 100ºC for 5 min before loading. The proteins were separated on a 4%–12% NuPAGE gel (Invitrogen) and transferred to a nitrocellulose (Schleicher & Schuell) membrane [40]. The membrane was blocked in 1× PBS, 0.1% Tween-20 (PBSTw) containing 10% (w/v) nonfat dry milk (NFDM, BioRad) for 1 hr at room temperature and incubated with α-GFP antibody (JL-8 1:1000 dilution, BD Biosciences) in PBSTw plus 5% (w/v) NFDM overnight at 4ºC. The membrane was washed in PBSTw 3 × 10 min and incubated with HRP-conjugated secondary (sheep α-mouse [Amersham, NA931V], 1:10,000 dilution) in PBSTw at room temperature for 1 hr, followed by three 10 min washes in PBSTw and ECL detection. Western blotting to detect MBP:MBK-2 in Figure 1A was performed as above with α-MBP antibody (#E8032S 1:10,000 dilution, NEB).

Generation of Phosphospecific MEI-1 Antibody, Western Blotting, and Immunostaining

Rabbit polyclonal antibody 129091/P3 was raised against peptide CAMTRQSGS(PO3)PEPPA and affinity purified (Bethyl Laboratories). For the western blot in Figure 2A, procedures were performed as in Immunoblotting, above, with the following antibodies and dilutions: 129091/P3 (1:2000), HRP-conjugated donkey anti-rabbit IgG (Jackson #711-035-152) (1:10,000). For immunostaining, embryos were fixed as described in [41] and incubated with 129091/P3 (1:2000 dilution) overnight at room temperature, followed by Alexa 568-conjugated goat anti-rabbit secondary antibody (1:250 dilution, Molecular Probes).

Microscopic Imaging and Quantitation

Images were acquired with a Hamamatsu ORCA-ER digital camera attached to a Zeiss Axioplan 2 equipped with Ludl shutters and

a mercury lamp. Pictures were acquired and processed with IPLab software (Scanalytics) and merged and cropped in Photoshop CS.

Images used for the graph in Figure 2C were collected with 0.125 s exposure, and in all cases, the raw pixel values were within the range of the CCD camera (0–4095). Using IPLab, we measured the average pixel intensity for a 70 × 70 pixel region within each embryo and corrected it for background staining by subtracting the average value obtained from 4-cell or older embryos on the same slide. Background-corrected values from three or more same-stage embryos (except cul-2(RNAi), Metaphase I where n = 1) were averaged and scaled such that the lowest average value (e.g., Metaphase I for P-MEI-1 staining) equals 0 and the maximal value (e.g., Pronuclear Formation for P-MEI-1 staining) equals 1. Embryos were staged by DAPI staining.

Supplemental Data

Supplemental Data include two figures and three tables and are available with this article online at: http://www.current-biology. com/cgi/content/full/16/1/■ ■ ■/DC1/.

References

1. DeRenzo, C., and Seydoux, G. (2004). A clean start: Degradation of maternal proteins at the oocyte-to-embryo transition. Trends Cell Biol. 14, 420–426.

2. Pang, K.M., Ishidate, T., Nakamura, K., Shirayama, M., Trzepacz, C., Schubert, C.M., Priess, J.R., and Mello, C.C. (2004). The mini-brain kinase homolog, mbk-2, is required for spindle positioning and asymmetric cell division in early C. elegans embryos. Dev. Biol. 265, 127–139.

3. Pellettieri, J., Reinke, V., Kim, S.K., and Seydoux, G. (2003). Coordinate activation of maternal protein degradation during the egg-to-embryo transition in C. elegans. Dev. Cell 5, 451–462.

4. Quintin, S., Mains, P.E., Zinke, A., and Hyman, A.A. (2003). The mbk-2 kinase is required for inactivation of MEI-1/katanin in the one-cell Caenorhabditis elegans embryo. EMBO Rep. 4, 1175–1181.

5. McNally, K.L., and McNally, F.J. (2005). Fertilization initiates the transition from anaphase I to metaphase II during female meiosis in C. elegans. Dev. Biol. 282, 218–230.

6. Campbell, L.E., and Proud, C.G. (2002). Differing substrate specificities of members of the DYRK family of arginine-directed protein kinases. FEBS Lett. 510, 31–36.

7. Himpel, S., Tegge, W., Frank, R., Leder, S., Joost, H.G., and Becker, W. (2000). Specificity determinants of substrate recognition by the protein kinase DYRK1A. J. Biol. Chem. 275, 2431–2438.

8. Rechsteiner, M., and Rogers, S.W. (1996). PEST sequences and regulation by proteolysis. Trends Biochem. Sci. 21, 267–271.

9. Detwiler, M.R., Reuben, M., Li, X., Rogers, E., and Lin, R. (2001). Two zinc finger proteins, OMA-1 and OMA-2, are redundantly required for oocyte maturation in C. elegans. Dev. Cell 1, 187–199.

10. Lin, R. (2003). A gain-of-function mutation in oma-1, a C. elegans gene required for oocyte maturation, results in delayed degradation of maternal proteins and embryonic lethality. Dev. Biol. 258, 226–239.

11. Clark-Maguire, S., and Mains, P.E. (1994). mei-1, a gene required for meiotic spindle formation in Caenorhabditis elegans, is a member of a family of ATPases. Genetics 136, 533–546.

12. Mains, P.E., Kemphues, K.J., Sprunger, S.A., Sulston, I.A., and Wood, W.B. (1990). Mutations affecting the meiotic and mitotic divisions of the early Caenorhabditis elegans embryo. Genetics 126, 593–605.

13. McCarter, J., Bartlett, B., Dang, T., and Schedl, T. (1999). On the control of oocyte meiotic maturation and ovulation in Caenorhabditis elegans. Dev. Biol. 205, 111–128.

14. Greenstein, D. (2005). Control of oocyte meiotic maturation and fertilization. In Wormbook, pp. 1–23, The C. elegans Research Community: http://www.wormbook.org.

15. L'Hernault, S.W., Shakes, D.C., and Ward, S. (1988). Developmental genetics of chromosome I spermatogenesis-defective mutants in the nematode Caenorhabditis elegans. Genetics 120, 435–452.

16. Singson, A., Mercer, K.B., and L'Hernault, S.W. (1998). The C. elegans spe-9 gene encodes a sperm transmembrane protein that contains EGF-like repeats and is required for fertilization. Cell 93, 71–79.

17. Boxem, M., Srinivasan, D.G., and van den Heuvel, S. (1999). The Caenorhabditis elegans gene ncc-1 encodes a cdc2-related kinase required for M phase in meiotic and mitotic cell divisions, but not for S phase. Development 126, 2227–2239.

18. Golden, A., Sadler, P.L., Wallenfang, M.R., Schumacher, J.M., Hamill, D.R., Bates, G., Bowerman, B., Seydoux, G., and Shakes, D.C. (2000). Metaphase to anaphase (mat) transition-defective mutants in Caenorhabditis elegans. J. Cell Biol. 151, 1469–1482.

19. Shakes, D.C., Sadler, P.L., Schumacher, J.M., Abdolrasulnia, M., and Golden, A. (2003). Developmental defects observed in hypomorphic anaphase-promoting complex mutants are linked to cell cycle abnormalities. Development 130, 1605–1620.

20. Liu, J., Vasudevan, S., and Kipreos, E.T. (2004). CUL-2 and ZYG-11 promote meiotic anaphase II and the proper placement of the anterior-posterior axis in C. elegans. Development 131, 3513–3525.

21. Sonneville, R., and Gonczy, P. (2004). Zyg-11 and cul-2 regulate progression through meiosis II and polarity establishment in C. elegans. Development 131, 3527–3543.

22. Nebreda, A.R., and Ferby, I. (2000). Regulation of the meiotic cell cycle in oocytes. Curr. Opin. Cell Biol. 12, 666–675.

23. Nash, P., Tang, X., Orlicky, S., Chen, Q., Gertler, F.B., Mendenhall, M.D., Sicheri, F., Pawson, T., and Tyers, M. (2001). Multisite phosphorylation of a CDK inhibitor sets a threshold for the onset of DNA replication. Nature 414, 514–521.

24. Nishi, Y., and Lin, R. (2005). DYRK2 and GSK-3 phosphorylate and promote the timely degradation of OMA-1, a key regulator of the oocyte-to-embryo transition in C. elegans. Dev. Biol., in press. Published online Nov. 10, 2005. 10.1016/j.ydbio.2005.09.053.

25. Shirayama, M., Soto, M.C., Ishidate, T., Kim, S., Nakamura, K., Bei, Y., van den Heuvel, S., and Mello, C.C. (2005). The conserved kinases CDK-1, GSK-3, KIN-19, and MBK-2 promote OMA-1 destruction to regulate the oocyte-to-embryo transition in C. elegans. Curr. Biol. 16, in press. Published online December 8, 2005. 10.1016/j.cub.2005.11.070.

26. Zou, Y., Ewton, D.Z., Deng, X., Mercer, S.E., and Friedman, E. (2004). Mirk/dyrk1B kinase destabilizes cyclin D1 by phosphorylation at threonine 288. J. Biol. Chem. 279, 27790–27798.

27. Deng, X., Mercer, S.E., Shah, S., Ewton, D.Z., and Friedman, E. (2004). The cyclin-dependent kinase inhibitor p27Kip1 is stabilized in G(0) by Mirk/dyrk1B kinase. J. Biol. Chem. 279, 22498–22504.

28. Deng, X., Ewton, D.Z., Mercer, S.E., and Friedman, E. (2005). Mirk/dyrk1B decreases the nuclear accumulation of class II histone deacetylases during skeletal muscle differentiation. J. Biol. Chem. 280, 4894–4905.

29. Mercer, S.E., Ewton, D.Z., Deng, X., Lim, S., Mazur, T.R., and Friedman, E. (2005). Mirk/Dyrk1B mediates survival during the differentiation of C2C12 myoblasts. J. Biol. Chem. 280, 25788–25801.

30. Voronina, E., and Wessel, G.M. (2003). The regulation of oocyte maturation. Curr. Top. Dev. Biol. 58, 53–110.

31. Santella, L., Lim, D., and Moccia, F. (2004). Calcium and fertilization: The beginning of life. Trends Biochem. Sci. 29, 400–408.

32. Brenner, S. (1974). The genetics of Caenorhabditis elegans. Genetics *77*, 71–94.

33. Timmons, L., Court, D.L., and Fire, A. (2001). Ingestion of bacterially expressed dsRNAs can produce specific and potent genetic interference in Caenorhabditis elegans. Gene *263*, 103–112.

34. Cuenca, A.A., Schetter, A., Aceto, D., Kemphues, K., and Seydoux, G. (2003). Polarization of the C. elegans zygote proceeds via distinct establishment and maintenance phases. Development *130*, 1255–1265.

35. Kamath, R.S., and Ahringer, J. (2003). Genome-wide RNAi screening in Caenorhabditis elegans. Methods *30*, 313–321.

36. DeRenzo, C., Reese, K.J., and Seydoux, G. (2003). Exclusion of germ plasm proteins from somatic lineages by cullin-dependent degradation. Nature *424*, 685–689.

37. Landy, A. (1989). Dynamic, structural, and regulatory aspects of lambda site-specific recombination. Annu. Rev. Biochem. *58*, 913–949.

38. Praitis, V., Casey, E., Collar, D., and Austin, J. (2001). Creation of low-copy integrated transgenic lines in Caenorhabditis elegans. Genetics *157*, 1217–1226.

39. Lochhead, P.A., Sibbet, G., Kinstrie, R., Cleghon, T., Rylatt, M., Morrison, D.K., and Cleghon, V. (2003). dDYRK2: A novel dual-specificity tyrosine-phosphorylation-regulated kinase in Drosophila. Biochem. J. *374*, 381–391.

40. Sambrook, J., Fritsch, E.F., and Maniatis, T. (1989). Molecular cloning: A Laboratory Manual, Second Edition, (Cold Spring Harbor, NY: Cold Spring Harbor Laboratory Press).

41. Guo, S., and Kemphues, K.J. (1995). par-1, a gene required for establishing polarity in C. elegans embryos, encodes a putative Ser/Thr kinase that is asymmetrically distributed. Cell *81*, 611–620.